Synthesis, Crystal Structure and Its Application in Living Cells Imaging of Benz(c)acridine-1,2,3-triazole Derivatives①

YAN Zhen-Shuo[a] KANG Yan-Hui[b]
CHEN Yang-Ling[a] HUO Li-Ni[a②]
[a] (*Guangxi University of Chinese Medicine, Nanning* 530001, *China*)
[b] (*Hebei University of Engineering, Handan* 056038, *China*)

ABSTRACT A highly selective iron ions fluorescent probe based on the benz(c)acridine-1,2,3-triazole derivatives was produced by multi-step reactions. 1-(7-Benz[c]acridinyl)-4-(4-methylphenyl)-1,2,3-triazole (**4a**), $C_{26}H_{18}N_4$, was structurally determined by single-crystal X-ray diffraction. It crystallizes in the trigonal system, space group *R*-3 with *a* = 36.230(10), *b* = 36.230(10), *c* = 7.993(3) Å, *β* = 90°, *V* = 9086(6) Å^3, *Z* = 18, D_c = 1.271 g/cm^3, *F*(000) = 3636, *μ* = 0.602 mm^{-1}, the final *R* = 0.0865 and *wR* = 0.1619 for 3951 observed reflections (*I* > 2*σ*(*I*)). X-ray analysis indicated that all four rings of benz(c)acridine are in the same plane, and the 1,2,3-triazole ring and the corresponding linked benzene (C(1)–C(6)–C(7)–C(8)–C(9)–N(1)) are approximately perpendicular with a dihedral angle of 106.5°. The crystal packing of the compound was stabilized by two weak interactions between C(11)–H(10)···N(4) and C(18)–H(18)···N(1). In fluorescence spectra studies, compound **4c** was exhibited good selectivity and sensitivity towards iron ions in DMSO: mops buffer solution. Furthermore, **4c** was successfully used for imaging iron ions in living HeLa cervical cancer cells.

Keywords: benz(c)acridine-1,2,3-triazole, crystal structure, fluorescent probe, iron ions;
DOI: 10.14102/j.cnki.0254-5861.2011-3159

1 INTRODUCTION

As the most abundant metal element in life systems, iron plays an indispensable role in living organisms, such as hematopoiesis, enzyme production, metabolic energy conversion, and immune function maintenance[1-3]. An abnormal concentration of iron ions in living systems would impair their normal physiological functions. Thus, it is necessary to develop highly selective and sensitive method to monitor Fe^{3+} both *in vivo* and *in vitro*. Compared with the traditional detection technology, fluorescent Fe^{3+} probes show advantages with higher sensitivity, faster responsiveness, as well as greater practicability[4].

In recent years, acridine derivatives have became the most promising optical materials owing to their large *π*-conjugated structures, good thermal stability, high luminous efficiency, and less background interference in some fields such as fluorescent probes, fluorescence sensor, and organic photoelectric device[5, 6]. Benz(c)acridine derivatives have four-ring conjugate plane and they might be performing well on fluorescence properties. But benz(c)acri- dine-type fluorescent probes are still reported rarely so far, and few of them have wide applications. Moreover, 1,2,3- triazole derivatives have received considerable attention because of their abundance electrons and good aromatic properties, leading to a wide range of applications in supramolecular chemistry[7]. The 1,2,3-triazole ring not only served as a linker through click chemistry, but also acted as a binding site for metal ions by hydrogen-bond interaction, coordinate bond, *π*-*π* stacking, etc[7, 8]. Therefore, 1,2,3-triazole unit is often introduced as a powerful and efficient ligation method in some fluorophore, some of which have been used

Received 25 February 2021; accepted 16 April 2021 (**CCDC 2062358**)

① Supported by the National Natural Science Foundation of China (No. 22067001), Natural Science Foundation of Guangxi Province (No. 2018GXNSFAA281189) and Graduate Education Innovation Project of Guangxi University of Chinese Medicine (No. YCSY20190027). We also thank the Guangxi Key Laboratory of *Zhuang* and *Yao* Ethnic Medicine ((2013) No. 20), Collaborative Innovation Center of *Zhuang* and *Yao* Ethnic Medicine ((2014) No. 32), Guangxi Key Discipline *Zhuang* Pharmacology ((2013) No. 16), First-class Discipline in Guangxi of traditional Chinese Pharmacology (Direction of Ethnic Medicine) ((2018) No. 12)

② Corresponding author. Born in 1982. Tel: +86-07714953513, E-mail: huolini@126.com

as fluorescence sensor[9, 10]. Based on this, 1,2,3-triazoles were introduced into benz(c)acridine skeleton in our studies for enhancing their fluorescence intensity or hydrophilicity with metal ions. All probes were characterized by ^{1}H NMR and HR-MS spectra, and manifested obviously selective to Fe^{3+} in the following experimental results.

2 EXPERIMENTAL

2. 1 Materials and methods

Commercially available chemicals were used in the experiment without further purification. All of them are reagents used in analytical reagent grade experiments. Various stock solutions of metal ions (Mn^{2+}, Mg^{2+}, Ag^{+}, Na^{+}, Ni^{2+}, Ca^{2+}, Cd^{2+}, Co^{2+}, Cu^{2+}, Fe^{3+}, Zn^{2+}, Pb^{2+}) were prepared in pure water (1×10^{-2} mol/L) with the corresponding perchlorate salts. The probes were dissolved in DMSO: mops buffer solution (pH = 6.9, 9:1(*v*/*v*)) to prepare the stock solutions with a concentration of 1.5×10^{-5} mol/L. The slight pH variations of the solutions were achieved by adding small volumes of NaOH or HCl. For all measurements, the excitation wavelength was 290 nm, and the excitation and emission slits were both set to 5.0 nm.

^{1}H-NMR spectra were recorded using chloroform-*d* with Bruker DRX-400 NMR instrument using TMS as internal standard. Mass spectra were recorded in Agilent 6210 ESI/TOF MS. The single-crystal X-ray was performed on a SuperNova, Dual, Cu at zero, AtlasS2 diffractometer. Melting point was determined on an X-4 micro melting point instrument. Fluorescence spectra were recorded on a Shimadzu RF-6000 fluorescence spectrophotometer equipped with a quartz cuvette with a path length of 1 cm. Confocal laser scanning microscopy (CLSM) imaging was taken on a confocal laser scanning biological microscope (Leica TCS SP5, German LEICA company).

2. 2 Synthesis of the title complex

Synthetic route of the title compounds is shown in Scheme 1.

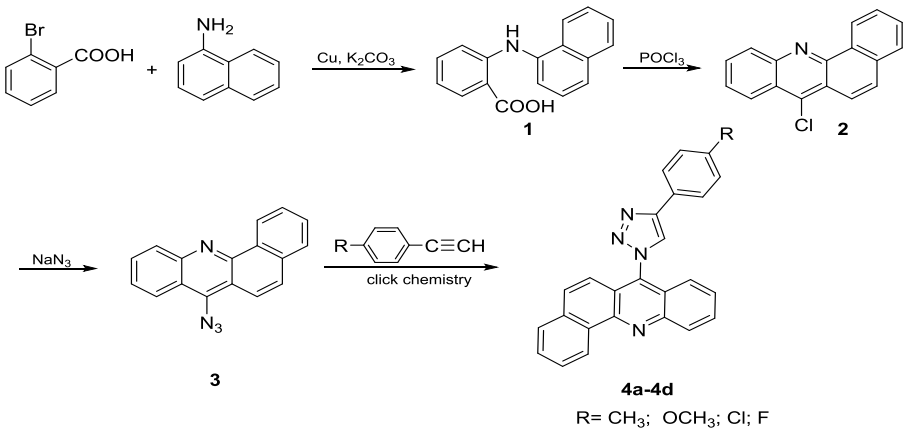

Scheme 1. Synthetic route of benz(c)acridine-1,2,3-triazole derivatives

2. 2. 1 Synthesis of N-phenyl-o-aminobenzoic acid (1) and 9-chlorine acridine (2)

The synthesis of the intermediate products (**1**) and (**2**) was according to the our reported procedure[11, 12].

N-phenyl-o-aminobenzoic acid (**1**): greenish yellow solid, yield 79%, m.p. 204.8～208.4 ℃. HR-MS(ESI) m/z: calcd. for $C_{17}H_{13}NO_2$ $[M+H]^+$: 264.1025, found: 264.1018. ^{1}H NMR (400 MHz, $CDCl_3$) δ 11.59 (s, 1H, -NH), 9.61 (s, 1H, ArH), 8.09 (d, *J* = 8.0 Hz, 2H, ArH), 7.91 (dd, *J* = 6.7, 2.6 Hz, 1H, ArH), 7.76 (d, *J* = 7.7 Hz, 1H, ArH), 7.56～7.48 (m, 3H, ArH), 7.28 (dd, *J* = 7.1, 1.5 Hz, 1H, ArH), 6.85 (d, *J* = 8.5 Hz, 1H, ArH), 6.76～6.71 (m, 1H, ArH).

9-Chlorine acridine (**2**): faint yellow needle crystals, yield 68%, m.p. 140.1～141.7 ℃; HR-MS(ESI) m/z: calcd. for $C_{17}H_{12}ClN$ $[M+H]^+$: 264.0577, found: 264.0580; ^{1}H NMR (400 MHz, $CDCl_3$) δ 9.50 (d, *J* = 7.8 Hz, 1H, ArH), 8.47 (d, *J* = 8.6 Hz, 1H, ArH), 8.37 (d, *J* = 8.6 Hz, 1H, ArH), 8.22 (d, *J* = 9.3 Hz, 1H, ArH), 7.88 (t, *J* = 8.1 Hz, 2H, ArH), 7.83 (d, *J* = 7.2 Hz, 1H, ArH), 7.80～7.75 (m, 2H, ArH), 7.73～7.68 (m, 1H, ArH).

2. 2. 2 Synthesis of probes 4a～4d by click chemistry

The probes **4a** ～ **4d** were prepared according to the documented procedure with slight modification[13]. Chlorine benz[c]acridine (1.49 g, 5.66 mmol) was dissolved in DMF (60 mL), followed by the addition of sodium azide (0.375 g, 5.77 mmol) and distilled water (30 mL). After heating to 100 ℃ and maintaining for 2 h, the reaction mixture was cooled at a 0 ℃ ice-bath for 60 min. The formed yellow-green

needle crystals were formed, filtered, washed with water, and dried in the air to give a pure intermediate **3** (yield 92.0%). **3** was directly used for the next step without further purification. Reaction of 7-azido benz[c]acridine (**3**, 1 mmol) with substituted phenylacetylene (2 mmol) in a mixture of 1:1 *t*-BuOH–H_2O in presence of $CuSO_4.5H_2O$ (0.04 g, 1.6 mmol) and sodium ascorbate (0.08 g, 0.4 mmol) at 80 ℃ for 3 h led to a precipitation which was filtered, washed with water, and recrystallized from chloroform to afford crystals **4a**～**4d**.

1-(7-Benz[c]acridinyl)-4-(4-methylphenyl)-1,2,3-triazole (**4a**): light yellow solid, yield 44%; m.p. 273.2～274.8 °C; HR-MS(ESI) m/z: calcd. for $C_{26}H_{18}N_4$ $[M+H]^+$: 387.1610, found: 387.1600; ^{1}H NMR (400 MHz, CDC1$_3$) δ 9.62 (d, J = 8.0 Hz, 1H, ArH), 8.56 (d, J = 8.7 Hz, 1H, ArH), 8.27 (s, 1H, -CH), 7.98～7.89 (m, 4H, ArH), 7.89～7.82 (m, 2H, ArH), 7.79 (d, J = 9.3 Hz, 1H, ArH), 7.67 (t, J = 7.6 Hz, 1H, ArH), 7.61 (d, J = 8.5 Hz, 1H, ArH), 7.37 (d, J = 7.8 Hz, 2H, ArH), 7.32 (d, J = 9.3 Hz, 1H, ArH), 2.47 (s, 3H, -CH_3).

1-(7-Benz[c]acridinyl)-4-(4-methoxyphenyl)-1,2,3-triazole (**4b**): light yellow solid, yield 40%; m.p. 263.9～265.8 ℃; HR-MS(ESI) m/z: calcd. for $C_{26}H_{18}N_4O$ $[M+H]^+$: 403.1559 , found: 403.1550; ^{1}H NMR (400 MHz, CDC1$_3$) δ 9.61 (d, J = 8.0 Hz, 1H, ArH), 8.54 (d, J = 8.7 Hz, 1H, ArH), 8.22 (s, 1H, -CH), 8.00 (d, J = 8.6 Hz, 2H, ArH), 7.97～7.90 (m, 2H, ArH), 7.85 (dd, J = 14.4, 8.0 Hz, 2H, ArH), 7.79 (d, J = 9.3 Hz, 1H, ArH), 7.71～7.59 (m, 2H, ArH), 7.33 (d, J = 9.3 Hz, 1H, ArH), 7.09 (d, J = 8.5 Hz, 2H, ArH), 3.93 (s, 3H, -OCH_3).

1-(7-Benz[c]acridinyl)-4-(4-chlorinephenyl)-1,2,3-triazole (**4c**): light yellow solid, yield 48%; m.p. 283.9～285.6 ℃; HR-MS(ESI) m/z: calcd. for $C_{25}H_{15}ClN_4$ $[M+H]^+$: 407.1032, found: 407.1043; ^{1}H NMR (400 MHz, CDC1$_3$) δ 9.65 (d, J = 7.2 Hz, 1H, ArH), 8.60 (d, J = 8.0 Hz, 1H, ArH), 8.31 (s, 1H, -CH), 8.01 (d, J = 8.3 Hz, 2H, ArH), 7.93 (q, J = 9.6, 8.0 Hz, 3H, ArH), 7.83 (dd, J = 19.1, 8.3 Hz, 2H, ArH), 7.69 (t, J = 7.6 Hz, 1H, ArH), 7.59 (d, J = 8.6 Hz, 1H, ArH), 7.54 (d, J = 7.9 Hz, 2H, ArH), 7.31 (s, 1H, ArH).

2-(7-Benz[c]acridinyl)-4-(4-fluorinephenyl)-1,2,3-triazole (**4d**): light yellow solid, yield 41%; m.p. 282.9～284.3 ℃; HR-MS(ESI) m/z: calcd. for $C_{25}H_{15}FN_4$ $[M+H]^+$: 391.1359, found: 391.1352; ^{1}H NMR (400 MHz, CDC1$_3$) δ 9.63 (d, J = 7.2 Hz, 1H, ArH), 8.57 (d, J = 8.2 Hz, 1H), 8.27 (s, 1H, -CH), 8.05 (s, 2H, ArH), 7.93 (d, J = 8.4 Hz, 2H, ArH), 7.90～7.82 (m, 2H, ArH), 7.80 (d, J = 9.4 Hz, 1H, ArH), 7.68 (t, J = 7.3 Hz, 1H, ArH), 7.60 (d, J = 8.5 Hz, 1H, ArH), 7.32 (s, 1H, ArH), 7.25 (d, J = 8.5 Hz, 2H, ArH).

2. 3 X-ray structure determination

A single crystal suitable for X-ray diffraction study was cultivated from chloroform and methyl alcohol by a slow evaporation method at room temperature. The colorless block crystal of **4a** having approximate dimensions of 0.13 × 0.12 × 0.11 mm^3. All measurements were performed with Cu$K\alpha$ radiation (λ = 1.54184 Å) on a SuperNova, Dual, Cu at zero, AtlasS2 diffractometer. Out of the 6952 total reflections collected in the range of 4.878 °≤2θ≤148.214 ° (–28≤h≤30, –27≤k≤44, –9≤l≤9) by using an ω scan mode, 3951 were independent with R_{int} = 0.1291, of which 2403 were observed with $I > 2\sigma(I)$ and used in the structure determination and refinements. The structure was solved by direct methods with SHELXS[14] and refined by SHELXL[15]. All non-hydrogen atoms were refined with anisotropic thermal parameters. The hydrogen atoms were placed in the calculated positions. The final full-matrix least-squares refinement gave R = 0.0865, wR = 0.2350 ($w = 1/[\sigma^2(F_o^2) + (0.0472P)^2]$, where $P = (F_o^2 + 2F_c^2)/3$), S = 0.942, $(\Delta\rho)_{max}$ = 0.30 and $(\Delta\rho)_{min}$ = –0.31 e/Å^3.

2. 4 Ion selectivity studies

The stock solutions of the probes **4a**～**4d** (1.5×10^{-5} mol/L) in DMSO: mops buffer solution (pH = 6.9, 9:1 (*v*/*v*)) and guest cations (1×10^{-2} mol/L) in ultrapure water were prepared. Fluorescence spectra were obtained by adding various amounts of cation solution to the probe solutions (3 mL). The fluorescence intensity was recorded at $\lambda_{ex}/\lambda_{em}$ = 290/424 nm alongside a reagent blank. The excitation and emission slits were both set to 5.0 nm.

The limit of detection was calculated based on the following equation:

Detection Limit (DL) = 3σ/k

where σ is the standard deviation of the blank measurement, and k is the slope of the graph of the relationship between fluorescence intensity and different metal ion concentrations.

2. 5 Celling imaging

HeLa cells were cultured in DMEM (Dulbecco's Modified Eagle Medium) containing 10% FBS (fetal bovine serum), and kept in a moist atmosphere containing 5% CO_2 at 37 ℃. The cytotoxiclty of probes **4a**～**4d** against HeLa cells was studied using a standard methyl thiazolyl tetrazolium (MTT) assay. Then, the cells were transferred to a 35 mm confocal dish in the culture medium for 24 h. For confocal fluorescence imaging, the cells were washed three times with PBS and incubated with probes **4a**～**4d** (10 μM in 1:100 DMSO-DMEM (*v*/*v*), pH = 7.4) in 2.0 mL. One group of cells was

treated with medium solution (in 1:100 DMSO-DMEM *v*/*v*, pH = 7.4) for 1 h, while another group was incubated with Fe^{3+} (0～100 μM in 1:100 DMSO-DMEM (*v*/*v*), pH = 7.4) for another 1 h. Cells were washed three times with PBS buffer solution to remove free compounds before imaging. After that, the cells attached to the confocal culture dish were observed with a confocal scanning system. The excitation wavelength was 290 nm and the fluorescence signals at 424 nm were collected.

3 RESULTS AND DISCUSSION

3. 1 Synthesis and characterization

The synthetic route used to prepare these four probes (**4a**～**4d)** is shown in Scheme 1. The synthesis of the benz(c)acridine skeleton (**2**) was through our previous studies[11]. The 1,2,3-triazole ring was introduced into 7-position of benz(c)acridine skeleton by click chemistry with moderate yield of 40～48%, which might be related to the terrible solubility of them. High temperature and long reaction time could not help to improve the yield of **4a**～**4d**. There were only a few products formed by TLC detection below 60 ℃. The optimum reaction condition has been explored in our previous studies such as reaction solvent, reaction time, reaction temperature, etc.[12]. The most appropriate temperature and reaction time were 80 ℃and 3 h, respectively. The resulted probes **4** were fully characterized by ^{1}H NMR and HR-MS spectroscopy. Compound **4a** was a colorless block crystal and stable in air at room temperature, and the molecular structure and the packing diagram of **4a** are depicted in Figs. 1 and 2.

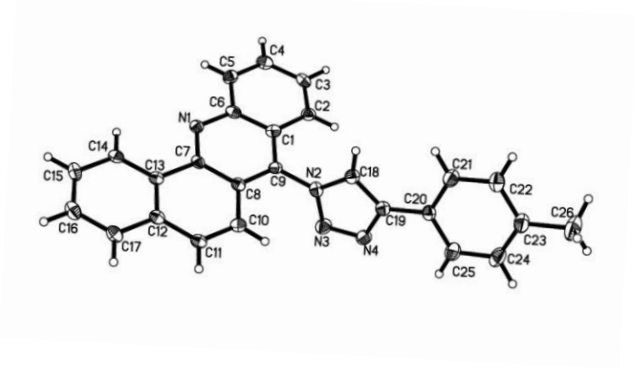

Fig. 1. X-ray crystal structure of probe 4a

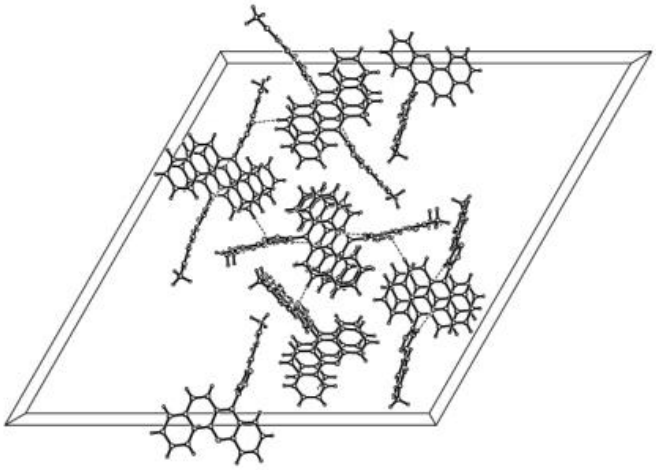

Fig. 2. Packing of probe 4a, viewed down the *c* direction. Dashed lines indicate hydrogen bonds

Compound **4a** crystallizes in the trigonal crystal system *R*-3 space group with one complete molecule in its asymmetric unit. The bond lengths and bond angles are in the expected ranges and described in Table 1. The C=N double bond lengths in the independent molecule are 1.351(7) Å (C(18)=N(2)) and 1.364(7) Å (C(19)=N(4)), respectively, exhibiting the double bond character. All four rings of benz(c)acridine are all in the same plane, with the N(1)–C(7)–C(13)–C(14) and C(4)–C(5)–C(6)–N(1) torsion angles to be 1.7(8)° and 179.2(5)°, respectively. Besides, the 1,2,3-triazole ring and the corresponding linked ring of benz(c)acridine (C(1)–C(6)–C(7)–C(8)–C(9)–N(1)) are

approximately perpendicular with a dihedral angle of 106.5°. And the ring of C(20)–C(25) and 1,2,3-triazole ring are nearly coplanar with a dihedral angle of 10.6°. In the crystal packing, the molecules are linked by two weak intermolecular interactions of C(11)–H(10)···N(4) (1/3–*x*, 2/3–*y*, 2/3–*z*) and C(18)–H(18)···N(1) (–1/3+*y*, 1/3–*x*+*y*, 4/3–*z*) hydrogen bonds by the distance of 3.506(9) and 3.270(8) Å, and the hydrogen bond data are shown in Table 2.

Table 1. Selected Bond Lengths (Å) and Bond Angles (°)

Bond	Dist.	Bond	Dist.	Bond	Dist.
N(2)–N(3)	1.357(6)	C(8)–C(7)	1.428(7)	C(20)–C(21)	1.393(8)
N(2)–C(9)	1.433(7)	C(8)–C(10)	1.443(7)	C(20)–C(25)	1.394(8)
N(2)–C(18)	1.351(7)	C(9)–C(1)	1.401(7)	C(17)–C(16)	1.390(8)
N(1)–C(7)	1.336(7)	C(12)–C(11)	1.420(8)	C(2)–C(3)	1.370(7)
N(1)–C(6)	1.370(7)	C(12)–C(17)	1.399(8)	C(5)–C(4)	1.372(8)
N(3)–N(4)	1.328(7)	C(1)–C(6)	1.412(8)	C(14)–C(15)	1.383(8)
N(4)–C(19)	1.364(7)	C(1)–C(2)	1.417(7)	C(3)–C(4)	1.416(8)
C(13)–C(12)	1.408(7)	C(19)–C(20)	1.453(8)	C(15)–C(16)	1.394(8)
C(13)–C(7)	1.455(7)	C(19)–C(18)	1.375(7)	C(22)–C(21)	1.380(8)
C(13)–C(14)	1.396(7)	C(6)–C(5)	1.416(7)	C(22)–C(23)	1.412(8)
C(8)–C(9)	1.380(7)	C(11)–C(10)	1.371(7)	C(23)–C24)	1.387(9)
C(23)–C(26)	1.510(8)	C(25)–C(24)	1.393(9)		
Angle	(°)	Angle	(°)	Angle	(°)
N(3)–N(2)–C(9)	120.6(5)	N(1)–C(7)–C(13)	118.1(5)	C(4)–C(5)–C(6)	119.7(6)
C(18)–N(2)–N(3)	111.7(5)	N(1)–C(7)–C(8)	122.0(5)	C(15)–C(14)–C(13)	120.0(5)
C(18)–N(2)–C(9)	127.6(5)	C(8)–C(7)–C(13)	119.9(5)	N(2)–C(18)–C(19)	105.1(5)
C(7)–N(1)–C(6)	119.0(5)	C(9)–C(1)–C(6)	117.3(5)	C(2)–C(3)–C(4)	120.5(6)
N(4)–N(3)–N(2)	105.3(5)	C(9)–C(1)–C(2)	123.2(5)	C(14)–C(15)–C(16)	120.2(6)
N(3)–N(4)–C(19)	110.6(5)	C(6)–C(1)–C(2)	119.6(5)	C(11)–C(10)–C(8)	120.7(5)
C(12)–C(13)–C(7)	118.3(5)	N(4)–C(19)–C(20)	122.8(5)	C(17)–C(16)–C(15)	119.9(6)
C(14)–C(13)–C(12)	120.6(5)	N(4)–C(19)–C(18)	107.3(5)	C(5)–C(4)–C(3)	120.7(5)
C(14)–C(13)–C(7)	121.0(5)	C(18)–C(19)–C(20)	129.9(6)	C(21)–C(22)–C(23)	121.1(7)
C(9)–C(8)–C(7)	118.3(5)	N(1)–C(6)–C(1)	122.5(5)	C(22)–C(21)–C(20)	121.2(6)
C(9)–C(8)–C(10)	122.7(5)	N(1)–C(6)–C(5)	117.9(5)	C(22)–C(23)–C(26)	120.4(7)
C(7)–C(8)–C(10)	119.0(5)	C(1)–C(6)–C(5)	119.6(5)	C(24)–C(23)–C(22)	117.1(6)
C(8)–C(9)–N(2)	119.8(5)	C(10)–C(11)–C(12)	120.7(5)	C(24)–C(23)–C(26)	122.5(6)
C(8)–C(9)–C(1)	120.9(5)	C(21)–C(20)–C(19)	120.9(5)	C(24)–C(25)–C(20)	120.6(7)
C(1)–C(9)–N(2)	119.3(5)	C(21)–C(20)–C(25)	118.1(6)	C(23)–C(24)–C(25)	121.8(6)
C(13)–C(12)–C(11)	121.2(5)	C(25)–C(20)–C(19)	121.0(6)		
C(17)–C(12)–C(13)	118.3(5)	C(16)–C(17)–C(12)	121.0(6)		
C(17)–C(12)–C(11)	120.5(5)	C(3)–C(2)–C(1)	119.9(6)		

Table 2. Hydrogen Bonds for Compound 4a (Å and °)

D–H···A	D–H	H···A	D···A	D–H···A
C(11)–H(10)···N(4)[a]	0.93	2.60	3.506(9)	163
C(18)–H(18)···N(1)[b]	0.93	2.45	3.270(8)	147

Symmetry codes: (a) 1/3–*x*, 2/3–*y*, 2/3–*z*; (b) –1/3+*y*, 1/3–*x*+*y*, 4/3–*z*

3. 2 Ion selectivity studies

The change in fluorescence emission of probes (**4a**～**4d**) toward different metal ions was then investigated in DMSO/mops buffer solution (9:1, *v*/*v*). As shown in Fig. 3, the addition of 10 equiv. of Mn^{2+} (Mg^{2+}, Ag^{+}, Na^{+}, Ni^{2+}, Ca^{2+}, Cd^{2+}, Co^{2+}, Zn^{2+}, Pb^{2+}) ion did not cause obvious change in the fluorescence spectra of **4a**～**4d**, while the addition of Cu^{2+} and Fe^{3+} ions could cause varying degrees of fluorescence quenching. Interestingly, the response was highly selective toward Fe^{3+} than Cu^{2+} ions for all these four probes. Besides, compound **4b** was sensitive to Zn^{2+} at the same time with slight fluorescence enhancement. In the same concentration, compound **4c** exhibited the most obvious fluorescence quenching at 424 nm with fluorescence

intensity decrease to 219705.5 (a.u.) from 288559.5 (a.u.). To further investigate the binding properties of **4c** with Fe^{3+} ions, spectral titrations were performed. Upon gradual addition of Fe^{3+} ions (up to 60-fold), the fluorescence emission at 424 nm decreased continuously accompanied by obvious fluorescence quenching (Fig. 4). The fluorescence intensity at 424 nm showed a linear relationship with the concentration of Fe^{3+} ions up to 0.3 mM (R^2 = 0.99556). The detection limit (DL) could be estimated to be 9.39 × 10^{-6} mM (σ = 1.61). Competition experiments were also performed by monitoring the change in fluorescence intensity of **4c** in the co-existence of common metal ions with Fe^{3+} ions (Fig. 5). Except for Cu^{2+} ions, it can be observed that the change was insignificant for probe **4c** when using most of the metal ions, which suggested that **4c** was highly selective toward Fe^{3+} ions and the binding affinity was too strong to be displaced by most of the common metal ions.

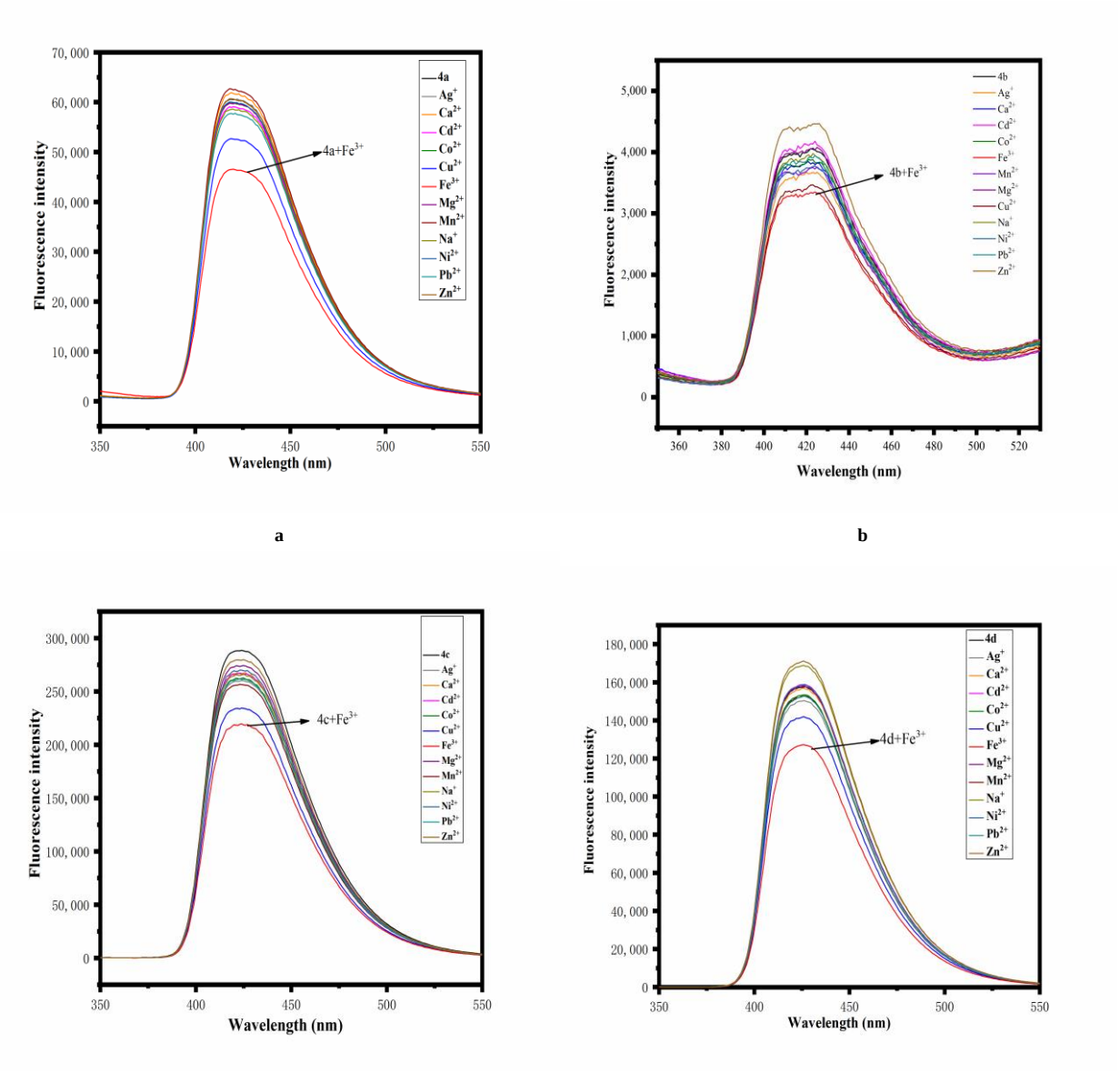

Fig. 3. Fluorescence responses of probes 4a∼4d (1.5 × 10^{-5} mol/L) toward different metal ions (1.0 × 10^{-2} mol/L)

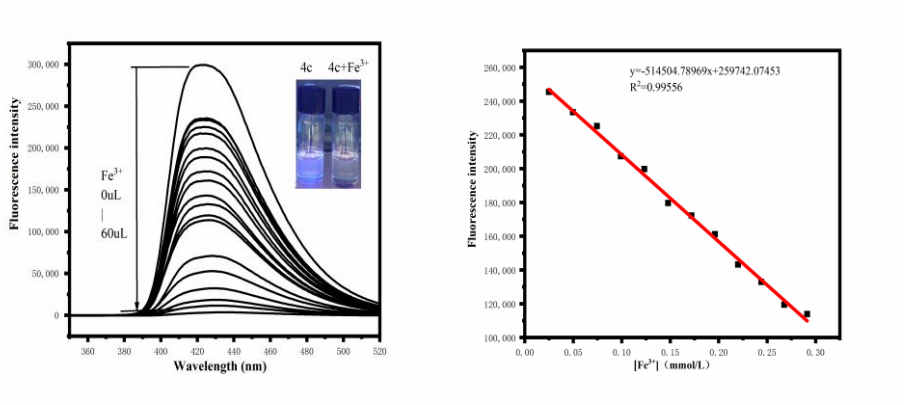

a **b**

Fig. 4. (a) Fluorescence response of probe 4c (1.5 × 10^{-5} mol/L) to different volume of Fe^{3+} (0 to 60 μL) in acetonitrile: mops buffer. (b) Linear correlation between concentration of Fe^{3+} (0 to 0.30 mM) and corresponding fluorescence intensities (λ_{ex} = 290 nm, λ_{em}: 424 nm, slit: 5 nm/5 nm)

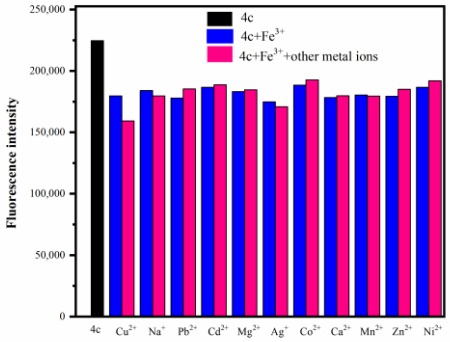

Fig. 5. Change in fluorescence intensity at 424 nm (4c, black) of a mixture of 4c (2 mm) and Fe^{3+} (20 equiv) in DMSO/mops buffer solution (9:1, v/v) upon the addition of different metal ions (20 equiv)

3. 3 Celling imaging studies

For testing the detection capability of Fe^{3+} in living cells of probe **4c**, confocal fluorescence microscope was used in the fluorescent imaging. As shown in Fig. 6, cells were first incubated with probe **4c** (10.0 μM) for about 20 min, and a very strong blue fluorescence inside the living HeLa cells was observed (Fig. 6a). Subsequently, the cells incubated with probe S were further pretreated with different concentrations of Fe^{3+} (0, 2.0, 10.0, 30.0, 50.0, 100.0 μM), and a significant gradient decrease in fluorescence intensity of the blue channel was observed (Figs. 6b～6e). After the final concentrations of Fe^{3+} reaching to 100 μM, there was no fluorescence from the intracellular area (Fig. 6f). The results revealed that probe **4c** could be potentially utilized as a biolabel to respond to Fe^{3+} in HeLa cells.

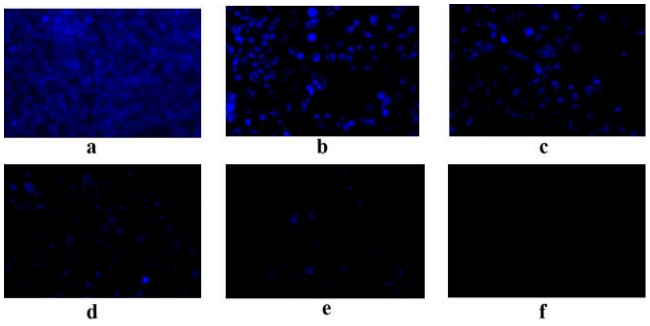

Fig. 6. Fluorescence images of HeLa cells incubated with the probe 4c (10.0 μM). Further incubated with the addition of Fe^{3+} (0, 2.0, 10.0, 30.0, 50.0, 100.0 μM, a～f) under 424 nm (The scale bar is 20 μm)

4 CONCLUSION

In summary, four benz[c]acridinyl-1,2,3-triazole derivatives (**4a** ~ **4d**) have been designed, synthesized and structurally characterized. The molecular structures and packing diagrams of **4a** showed that the molecules stabilized by two weak intermolecular interactions. The fluorescent spectral experiments indicated that all probes especially **4c** have excellent selectivity and sensitivity toward Fe^{3+}. The results of competitive experiments further confirmed its outstanding selectivity in the presence of other common metal ions (except for Cu^{2+} ions). The detection limit of the probe **4c** to Fe^{3+} was 9.39×10^{-6} mM. The fluorescent microscopy experiments demonstrated that probe **4c** could be used to investigate biological processes involving Fe^{3+} within living cells. These results provide further insight into developing novel fluorescent probes based on benz(c)acridine skeleton.

REFERENCES

(1) Raymond, K. N.; Dertz, E. A.; Kim, S. S. Enterobactin: an archetype for microbial iron transport. *Proc. Natl. Acad. Sci. U.S.A* **2003**, 100, 3584−3588.

(2) Pantopoulos, K.; Porwal, S. K.; Tartakoff, A.; Devireddy, L. Mechanisms of mammalian iron homeostasis. *Biochemistry* **2012**, 51, 5705−5724.

(3) Abbaspour, N.; Hurrell, R.; Kelishadi, R. Review on iron and its importance for human health. *J. Res. Med. Sci.* **2014**, 19, 164−174.

(4) Kindra, L. R.; Eggers, C. J.; Liu, A. T.; Mendoza, K.; Mendoza, J.; Myers, A. R. K.; Penner, R. M. Lithographically patterned PEDOT nanowires for the detection of iron(III) with nanomolar sensitivity. *Anal. Chem.* **2015**, 87, 11492−11500.

(5) Guo, C. H.; Hsu, G. S. W.; Chuang, C. J.; Chen, P. C. Aluminum accumulation induced testicular oxidative stress and altered selenium metabolism in mice. *Environ. Toxicol. Pharmacol*. **2009**, 27, 176−181.

(6) Li, Q.; Song, P.; Dai, Y.; Wang, C.; Xu, K. Progress in fluorescent chemical sensors based on acridine. *Chem. Res.* **2015**, 26, 433−440.

(7) Lau, Y. H.; Rutledge, P. J.; Watkinson, M.; Todd, M. H. Chemical sensors that incorporate click-derived triazoles. *Chem. Soc. Rev.* **2011**, 40, 2848−2866.

(8) Ng, D. K. P.; Shi, W. J.; Liu, J. Y.; Lo, P. C. Selective detection of Hg^{2+} ion with boron dipyrromethene-based fluorescent probes appended with a bis(1,2,3-triazole)amino receptor. *Chem. Asian J.* **2019**, 14, 1059−1065.

(9) Xiao, L.; Ren, P.; Jing, X.; Ren, L.; Li, Z.; Dai, F. Application in molecular recognition of 1,2,3-trizole derivatives. *Chin. J. Org. Chem.* **2017**, 37, 3085−3095.

(10) Chen, Y.; Zheng, C.; Peng, X.; Fu, Q.; Wu, L.; Lin, Q. Research progress in the synthesis of 1,2,3-triazole under transition-metal-free. *Chin. J. Org. Chem.* **2016**, 36, 1779−1789.

(11) Chen, R.; Huo, L. N.; Jaiswal, Y.; Huang, J. Y.; Zhong, Z. G.; Zhong, J.; Leonard, W.; Xia, X.; Liang, Y.; Yan, Z. S. Design, synthesis, antimicrobial, and anticancer activities of acridine thiosemicarbazides derivatives. *Molecules* **2019**, 24, 2065−15.

(12) Huo, L. N.; Chen, R.; Li, P. Y.; Su, W.; Lu, R. M. The preparation method of 1-(7-benz[c]acridinyl)-4-(4-methylphenyl)-1,2,3-triazole. *CN Patent, C07D401/04*. 2015108702191. 2016−03−23.

(13) Huo, L. N.; Chen, R.; Liao, Y. F.; Liu, H. G.; Li, P. Y.; Lu, R. M.; Zhong, Z. G. Synthesis, crystal structure and biological evaluation of acridine-1,2,3-triazole derivatives. *Chin. J. Struct. Chem.* **2016**, 35, 698−704.

(14) Sheldrick, G. M. A short history of SHELX. *Acta Cryst*. **2008**, A64, 112−122.

(15) Sheldrick, G. M. Crystal structure refinement with SHELXL. *Acta Cryst.* **2015**, C71, 3−8.